ELSEVIER

Polymer 41 (2000) 6161–6169

polymer

Ab initio study of hydrogenolysis as a chain transfer mechanism in olefin polymerization catalyzed by metallocenes

J. Ramos[a], V. Cruz[b], A. Muñoz-Escalona[c], J. Martínez-Salazar[a,*]

[a]*GIDEM, Instituto de Estructura de la Materia, CSIC Serrano 119, 28006 Madrid, Spain*
[b]*CTI, CSIC Pinar 21, 28006 Madrid, Spain*
[c]*Repsol I + D, Embajadores 183, 28045 Madrid, Spain*

Received 26 September 1999; accepted 5 November 1999

Abstract

Hydrogenolysis is a commonly used method to control the molecular weight or size of polymers obtained by Ziegler–Natta and related metallocene catalysts. However, the precise mechanism governing these controlling processes is still unknown. It is most accepted that the insertion of hydrogen molecule into the metal–alkyl bond of the catalyst active species competes favorably against the ethylene insertion. Thus, the newly formed hydride complex would react with an incoming ethylene starting a new polymer chain. Ab initio calculations at the B3LYP/LANL2DZ level of theory have been performed to calculate the reaction profile of both ethylene and hydrogen insertions into the metal–carbon bond of a zirconocene catalyst system. It has been observed that the activation barrier for the hydrogen molecule insertion is lower than that in case of the ethylene insertion (4.58 vs 7.48 kcal/mol), supporting the idea of a favored hydrogenolysis process controlling the molecular weight of the polymers. In addition, the ethylene insertion into the hydride complex formed after hydrogenolysis was also studied. No barrier for this reaction has been found, indicating that the initiation of a new chain is an easy step from both thermodynamic and kinetic points of view. The energetic data obtained in the present work provide a reasonable explanation for some experimental facts such as broadening of polymer molecular weight distributions and the early consumption of hydrogen present in the ethylene polymerization.

Keywords: Ethylene; Hydrogen; Hydrogenolysis

1. Introduction

Ziegler–Natta catalysts have been used for more than 40 years in the polyolefin production but it is only recently that the different issues concerning olefin polymerization by means of Ziegler–Natta catalysts have been tackled by quantum chemical methods. For instance, the mechanism of ethylene insertion in the metal–alkyl bond [1–4], termination chain reactions [5–8], regio and stereoselectivity of propylene polymerization [9], the comonomer effect [10], the influence of different ligands coordinated to a metal center [11,12] or the effect of two ethylene molecule on the insertion of ethylene in zirconocene catalyst [13] captured the interest of different laboratories. However, the effect of the addition of molecular hydrogen to the reactor, a widely used industrial method for the control of the polymer molecular weights obtained with Ziegler–Natta catalysts [14–24], has received much less attention. On the other hand, the ethylene and propylene polymerization with Ziegler–Natta heterogeneous catalysts has been extensively studied [14–20] due to its industrial importance. It has been experimentally observed that the activity of the heterogeneous catalyst increases when the propylene polymerization is carried out in the presence of molecular hydrogen. This fact has been explained by considering that the hydrogen chain transfer reactions would renew "dormant" sites in the catalyst, coming from isolated secondary insertions [14–20]. On the contrary, for the ethylene polymerization the changes in the catalyst activity due to the presence of molecular hydrogen have not been yet satisfactorily explained [14,16,18]. In fact, the effect of molecular hydrogen on the catalytic activity of metallocene catalysts has received poor attention. Some work has been done on the polymerization of propylene in the presence of hydrogen using different metallocenes as catalysts [21–23]. In all the reported cases, it appears that the catalytic activity increases when hydrogen is present at the reactor. This fact is explained again by the renewing of "dormant" sites produced by the molecular hydrogen [21–23]. The analysis of chain-end groups has given some support to this idea, but

* Corresponding author.

0032-3861/00/$ - see front matter
PII: S0032-3861(99)00827-7

is not conclusive [21]. Surprisingly, only a few numbers of papers related to the ethylene polymerization with metallocene catalysts in the presence of hydrogen have been published [24–27] although the changes of the catalyst have not been properly explained by these works.

Recently, Blom and Dahl [24] have reported some results obtained on the ethylene polymerization in the presence of molecular hydrogen using the metallocene Cp_2ZrCl_2 catalyst. It seems that the Cp_2ZrCl_2 catalyst showed a very high reactivity towards hydrogen. By performing a series of polymerization reactions in which the hydrogen was constantly introduced in the reactor at different flow rates ranging from 6 to 60 ml/min, they did not observe a systematic activity change vs the constant hydrogen flow. At low hydrogen flow a decrease of catalyst activity was obtained, but this tendency is reversed towards higher activities when the hydrogen flow is increased. Furthermore, it has been experimentally observed that the presence of molecular hydrogen produces a broadening of the polymer molecular weight distribution [24–27].

Some theoretical works have studied the ethylene insertion into the metallocene hydride complex in order to investigate the formation of a new polymer chain [28,29]. Zakharov et al. [28] have calculated the activation barrier for the ethylene insertion into H_2TiR^+ ($R = CH_3$, H) at MP2/3-21G* level of theory. The energy barrier obtained for the ethylene insertion into $H_2TiCH_3^+$ (about 18.0 kcal/mol) is higher than the insertion into H_2TiH^+ (about 3.0 kcal/mol). Hyla-Kryspin et al. [29] have studied the reaction of acetylene with the model compound $Cl_2ZrCH_3^+$ at RMP2/RHF level of theory. They observed a small energy barrier (0.2 kcal/mol) and a large exothermicity (−8.69 kcal/mol) for the acetylene insertion into Cl_2ZrH^+ suggesting that the reaction of acetylene into the Zr–H bond should be irreversible. They found an energy barrier of 5.1 kcal/mol for the acetylene insertion into the $Cl_2ZrCH_3^+$ cation.

In this work we performed ab initio calculations at B3LYP/LANL2DZ level to calculate the reaction profile of both ethylene and hydrogen insertion into zirconocene catalyst to shed light on the effect of molecular hydrogen on ethylene insertion into these catalyst active centers. Additionally, we have studied the ethylene insertion into the hydride complex formed after hydrogenolysis reaction in order to check the possibility of the formation of a new polymer chain.

The main goal of the present work is then to give a reasonable explanation for some experimental facts for the ethylene polymerization process in the presence of hydrogen with metallocene catalyst systems, as it is the early consumption of molecular hydrogen and the broadening of polymer molecular weight distribution.

2. Computational methods

Geometries, energies and vibrational frequencies for the reactants, transition states and products of the different reactions were calculated with the GAUSSIAN98 package [30], under the B3LYP DFT hybrid model [31], which has been shown to be quite reliable in both geometry and energy calculations [32].

This method includes a mixture of Hartree–Fock and DFT exchange in addition to DFT correlation terms and takes the form:

$$E_{\mathrm{B3LYP}}^{\mathrm{XC}} = A \times E_{\mathrm{X}}^{\mathrm{Slater}} + (1 - A) \times E_{\mathrm{X}}^{\mathrm{HF}} + B \times \Delta E_{\mathrm{X}}^{\mathrm{B88}} + E_{\mathrm{C}}^{\mathrm{VWN}} + C \times \Delta E_{\mathrm{C}}^{\mathrm{LYP}}$$

The local correlation terms are given by the Vosko et al. [33] ($E_{\mathrm{C}}^{\mathrm{VWN}}$) and Lee et al. [34] ($\Delta E_{\mathrm{C}}^{\mathrm{LYP}}$) functionals, the latter including the non-local correction terms. The exchange terms are given by a combination of Slater ($E_{\mathrm{X}}^{\mathrm{Slater}}$) [35] and Becke ($\Delta E_{\mathrm{X}}^{\mathrm{B88}}$) [36] exchange functional in addition to the Hartree–Fock one ($E_{\mathrm{X}}^{\mathrm{HF}}$). The *A*, *B* and *C* constants were determined by Becke by fitting to the G1 molecule set.

The LANL2DZ (Los Alamos ECP plus DZ) [37–39] basis set was used for all atoms. This basis set makes use of effective core potentials for the innermost electrons and takes into account some relativistic effects in post-third-row atoms.

The transition state geometries were obtained by the STQN (synchronous transit-guided quasi-Newton) [40] method to locate a saddle-point in the path from reactant to product. Frequency calculations were performed in order to check the nature of the stationary points found.

The calculation of some thermodynamic data was performed at 298.15 K and 1 atm of pressure using standard statistical thermodynamic methods implemented in GAUSSIAN98 package. The imaginary frequencies for the transition states were neglected in all the calculations. No symmetry constraints were used.

The evaluation of relative population was based assuming Boltzmann statistics and using the standard equation:

$$\frac{n_i}{N} = \frac{\exp(-G_i/\mathrm{k}T)}{\sum_j \exp(-G_j/\mathrm{k}T)}$$

where n_i is the population in energy level *i*, *N* the total population, G_i the Gibbs free energy corresponding to level *i*, k the Boltzmann constant and *T* is the absolute temperature. The n_i/N ratio is related to the probability of finding a molecule at energy level *i*. Equilibrium conditions are assumed for the application of the statistical thermodynamics, although the experimental work [24–27] was not supposed to be a priori in the equilibrium state. The initial structures were built with Spartan package [41] in a Silicon Graphics workstation.

3. Results and discussion

All the reactions studied in the present work are

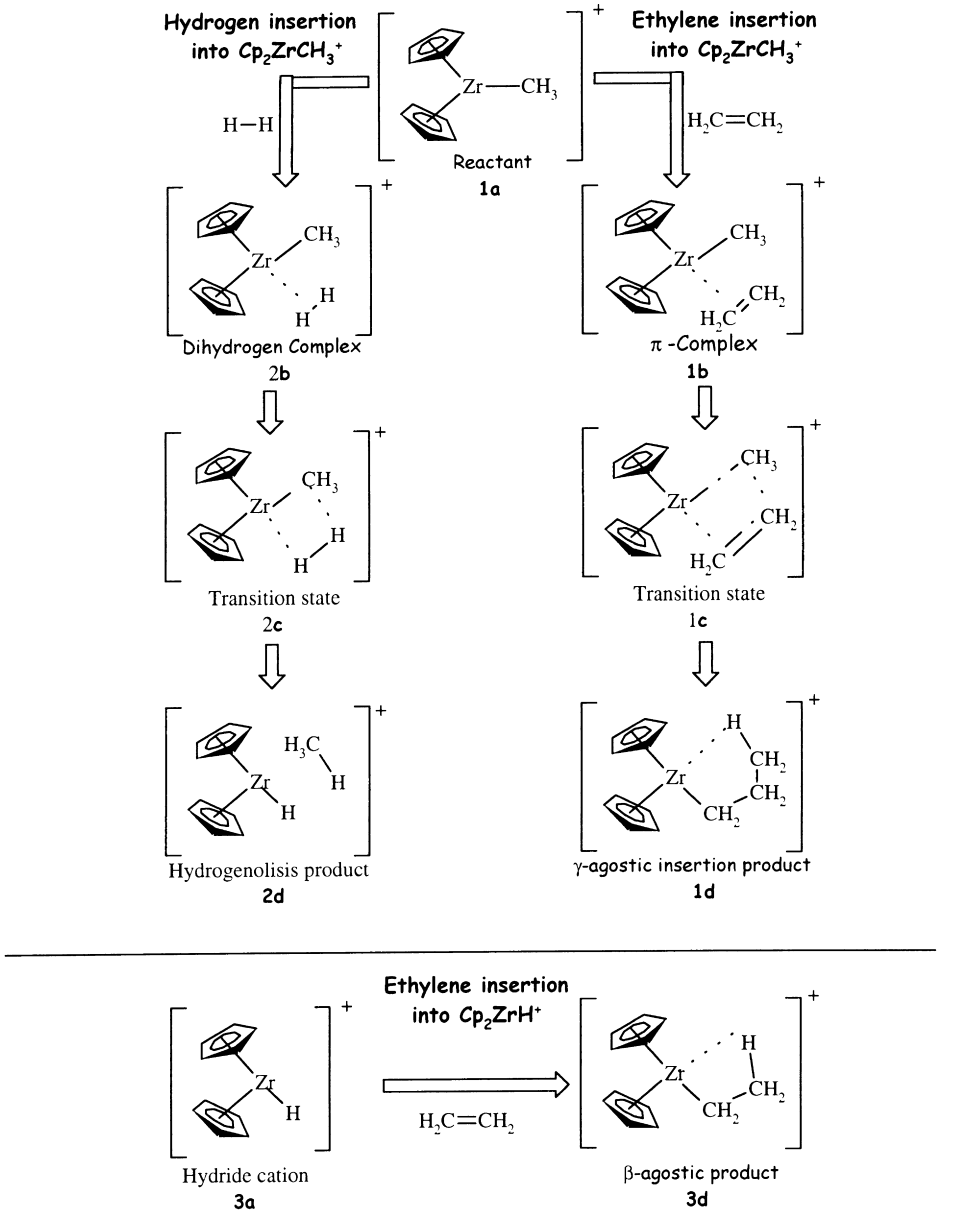

Scheme 1.

Table 1
Main geometrical parameters for reactants (**1a** + ethylene), π-complex (**1b**), TS (**1c**), and products (**1d**) of ethylene insertion into $Cp_2ZrCH_3^+$. The labels are defined in Fig. 1 (distances are in Å and angles in °)

	Reactants (**1a** + ethylene)	π-complex (**1b**)	Transition state (**1c**)	Product (**1d**)[a]
Zr–C1	–	2.966	2.376	2.221
Zr–C2	–	2.838	2.669	2.743
Zr–Cα	2.230	2.243	2.327	2.719
Zr–Hα	2.799	2.873	2.198	2.328
C1–C2	1.348	1.362	1.432	1.577
C2–Cα	–	3.413	2.168	1.576
Zr–Cα–Hα	109.6	114.1	69.5	58.0
Cp–Zr–Cp	136.2	132.3	133.8	132.9
Zr–Cα–C2–C1	–	33.4	−6.1	−29.5

[a] The C1, C2, Cα, Hα atoms are renamed in the product as Cα, Cβ, Cγ and Hγ, respectively (see Fig. 1).

Table 2
Main geometrical parameters for reactants (**1a** + hydrogen), dihydrogen complex (**2b**), TS (**2c**), and products (**2d**) of hydrogen insertion into $Cp_2ZrCH_3^+$. The labels are defined in Fig. 2 (distances are in Å and angles in °)

	Reactants (**1a** + ethylene)	Dihydrogen complex (**2b**)	Transition state (**2c**)	Product (**2d**)
Zr–H1	–	2.376	1.958	1.820
Zr–H2	–	2.376	1.955	3.410
Zr–Cα	2.230	2.233	2.350	2.779
Zr–Hα	2.799	2.805	2.413	2.426
H1–H2	0.743	0.759	0.950	2.336
H2–Cα	–	3.351	1.558	1.110
Zr–Cα–Hα	109.6	113.8	79.6	–
Cp–Zr–Cp	136.2	135.5	137.1	136.5
Zr–Cα–H2–H1	–	−83.5	0.3	6.1

summarized in the Scheme 1. Both the ethylene and hydrogen insertion processes into a $Cl_2ZrCH_3^+$ model catalyst have been considered and studied with the B3LYP/LANL2DZ theoretical approach. The hydrogen insertion (**2b**) into the metal–alkyl bond (hydrogenolysis) is competitive against the ethylene insertion (**1b**) into the same bond. The ethylene insertion mechanism into the hydride complex (**3a**) formed by hydrogenolysis was also followed with the same theoretical model in order to check whether the formed hydride complex (**3a**) is an active center for the ethylene insertion and therefore could start a new polymer chain. The structures for stationary points and energy profiles as well as some thermodynamic calculations were obtained for all processes and will be discussed in the following sections.

3.1. Geometries

In order to explore the competition between ethylene insertion and hydrogen insertion in the same model catalyst (**1a**) we have optimized reactants (**1a**, **3a**), binding complexes (**1b**, **2b**), transition states (**1c**, **2c**) and products (**1d**, **2d**, **3d**) for both insertions. The main geometrical parameters for the ethylene insertion and hydrogen insertion into the $Cp_2ZrCH_3^+$ model catalyst are shown in Tables 1 and 2, respectively. Analogously, the geometrical parameters for ethylene insertion into the Cp_2ZrH^+ are displayed in Table 3. The corresponding labels are represented in Figs. 1–3.

Table 3
Main geometrical parameters for reactants (**3a** + ethylene) and products (**3b**) of ethylene insertion Cp_2ZrH^+. The labels are defined in Fig. 3 (distances are in Å and angles in °)

	Reactants (**3a** + ethylene)	Product (**3d**)[a]
Zr–Hα	1.813	2.207
Zr–C1	–	2.236
Zr–C2	–	2.629
C1–C2	1.348	1.536
Zr–C1–C2	–	86.3
Cp–Zr–Cp	138.1	136.9
Zr–C1–H2–H1	–	0.0

[a] The C1, C2, Hα atoms are renamed in the product as Cα, Cβ, Hβ, respectively (see Fig. 3).

Considering first the reactants, the optimized structure of **1a** may be compared with the experimental X-ray structure of the complex $\{[1,2\text{-}Me_2Cp]_2ZrCH_3^+ \ CH_3B(C_5F_5)_3^-\}$ [42], being in reasonable agreement with it.

For the measurement of the agostic interaction the Zr–H distances and Zr–C–H angles are generally used. Some authors have showed that these geometrical parameters are adequate to analyze these interactions [8,9]. In the optimized structure of the cationic reactant (**1a**) we have not found any α-agostic interaction as deduced from the $Zr–H_\alpha$ distances (2.799 Å) and $Zr–C_\alpha–H_\alpha$ angles (109.6°), which are in agreement with the data published by Ziegler's group [8]. By using the LDA-DF (local density approximation density functional) level they obtained negligible α-agostic interaction for the $Cp_2ZrCH_3^+$ structure.

Regarding the binding complexes, the main geometrical parameters for the optimized structures of the ethylene π complex (**1b**) and dihydrogen complex (**2b**) are presented in Tables 1 and 2. None of them exhibited an α-agostic interaction. The main difference between these binding complex structures (**1b** and **2b**) is based on how the ethylene and hydrogen molecules, respectively, approach the zirconium atom. The ethylene coordination to the Zr atom is not symmetric (distance Zr–Cl 2.966 Å and Zr–C2 2.838 Å) while the hydrogen is clearly symmetric (distance Zr–H1 and Zr–H2, 2.376 Å). On the other hand, the orientation of ethylene atoms (C1 and C2) and hydrogen atoms (H1 and H2) with respect to Zr–Cα bond is different as deduced from the dihedral angle values, Zr–Cα–C2–C1 (33.4°) and Zr–Cα–H2–H1 (−83.5°). In the dihydrogen complex (**2b**) the Zr–Cα and the H–H bonds are mutually perpendicular while in the ethylene π complex the ethylene molecule is approximately in the same plane as the Zr–Cα bond (compare **1b** and **2b** in Figs. 1 and 2, respectively).

In the binding complexes (**1b**, **2b**), the Zr–Cα distances are very similar to those obtained for the cationic reactants (**1a**). The Cp centroid–Zr–Cp centroid angle is reduced from 136.3° in the cationic reactant (**1a**) to 132.3° in the formation of the π-complex (**1b**) giving more room for the incoming ethylene molecule. This angle reduction

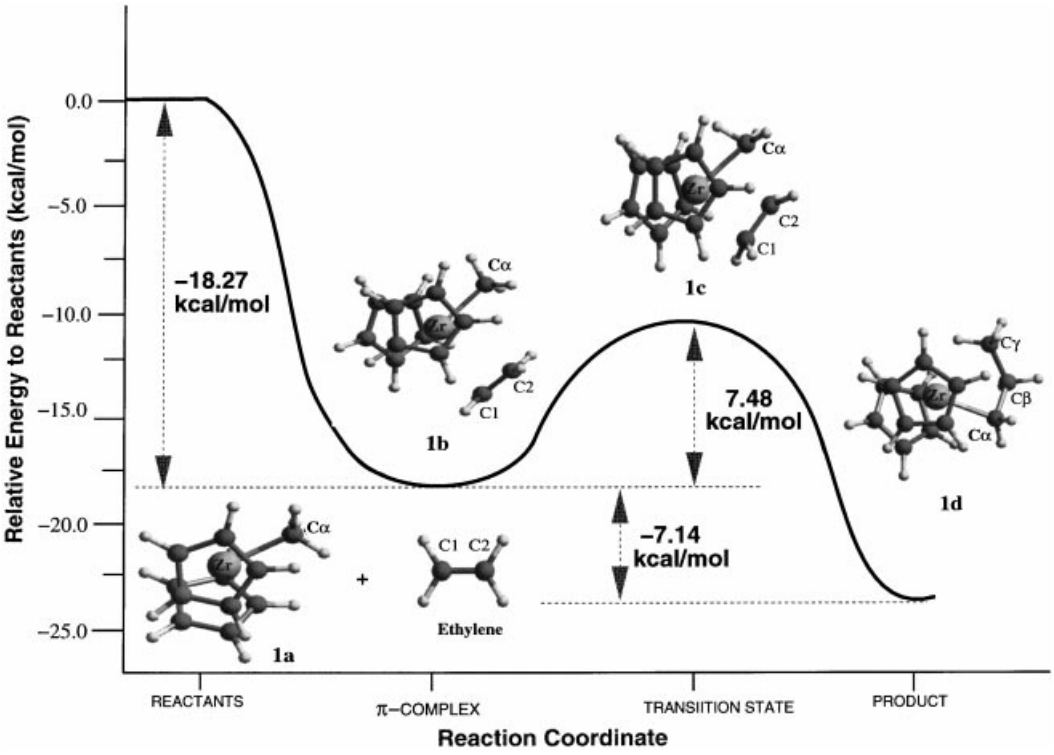

Fig. 1. Selected geometries and energy profile relative to reactant energies for the ethylene insertion into $Cp_2ZrCH_3^+$ (**1a**).

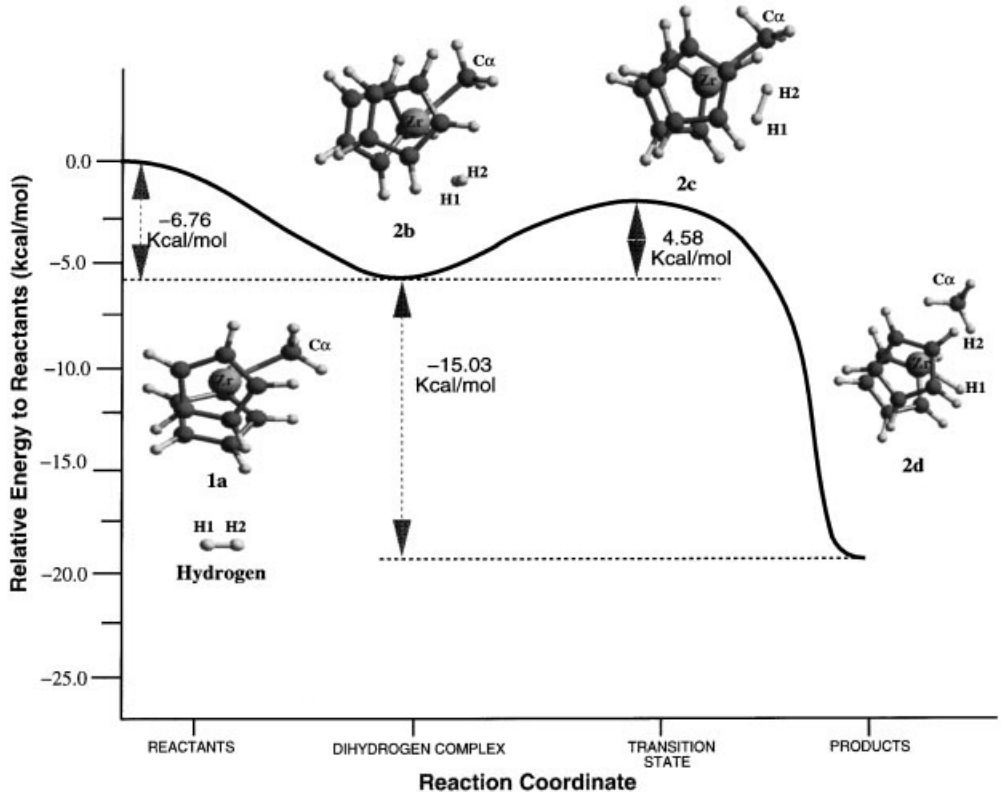

Fig. 2. Selected geometries and energy profile relative to reactant energies for the hydrogen insertion into $Cp_2ZrCH_3^+$ (**1a**).

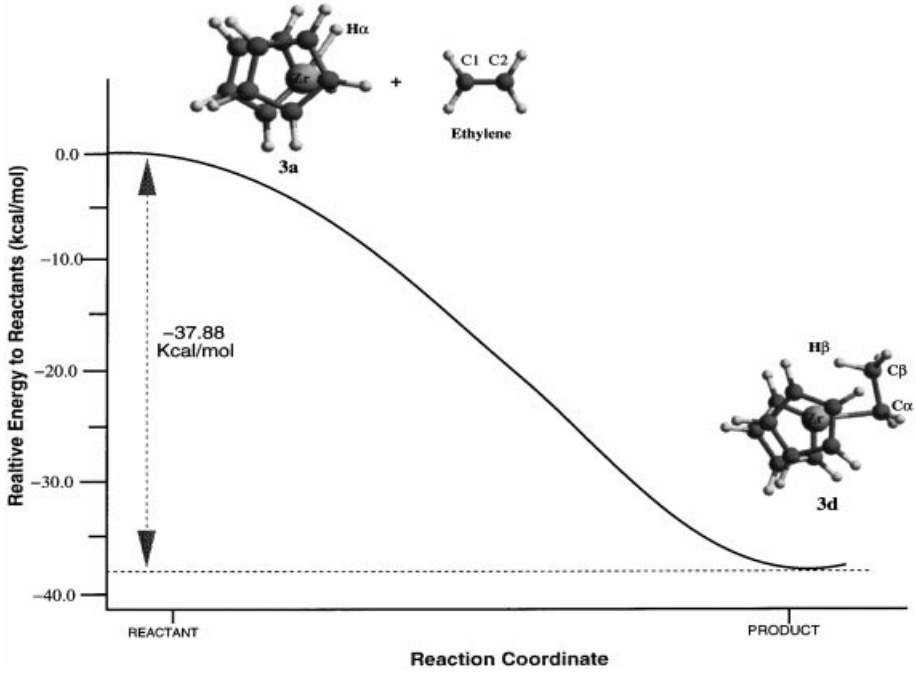

Fig. 3. Selected geometries and energy profile relative to reactant energies for the ethylene insertion into Cp_2ZrH^+ (**3a**).

practically was not observed in the formation of the dihydrogen complex (**2b**) (1.36.3° for reactants vs 135.7° for the dihydrogen complex). This observation could be explained by the different steric interactions between the hydrogen or ethylene molecules with the cyclopentadienyl ligands.

The transition state geometries for the ethylene insertion (**1c**) and the hydrogen insertion (**2c**) corresponds to the four-membered ring postulated by the Cosee–Arlman mechanism [43]. On the other hand, it is also observed that both insertions are assisted by α-agostic interaction in agreement with the Brookhart–Green mechanism [44]. The four atoms involved in the reactions are practically placed in the same plane as showed by the dihedral angles Zr–Cα–C2–C1 (−6.1°) and Zr–Cα–H2–H1 (0.3°).

The transition state geometry for the ethylene insertion (**1c**) occurs relatively earlier in the reaction path than the transition state for the hydrogen insertion (**2c**). The C1–C2 distance has only been increased by 0.070 Å and the Zr–Cα bond has elongated 0.084 Å in the transition state **1c** while the H1–H2 and Zr–Cα bonds have been increased by 0.191 and 0.117 Å, respectively, in the transition state **2c**.

The α-agostic interaction in the transition state **1c** is stronger than in the transition state **2c** (2.198 Å Zr–Hα in **1c** vs 2.413 Å Zr–Hα in **2c**) so that ethylene insertion is more clearly assisted by an α-agostic interaction.

In the case of the ethylene insertion into the hydride complex formed by the hydrogenolysis reaction neither π-complex nor transition state were found (Fig. 3). It can be observed that the ethylene molecule inserts spontaneously into the Zr–H bond of the cation hydride reactant (**3a**).

The product formed by the ethylene insertion into $Cp_2ZrCH_3^+$ (**1d**) presents a γ-agostic interaction (Zr–Hγ distance 2.328 Å). This γ-agostic interaction is apparently weaker than the one found by Ziegler et al. using LDA-DF model where the Zr–Hγ distance is shorter (Zr–Hγ distance 2.04 Å) [8]. It is known that the LDA-DF methods overestimate agostic interactions [7]. Furthermore, in structure **1d** it is observed that on going from transition structure (**1c**) to the product (**1d**) the Cα–Cβ bond distance is somehow elongated to reach a value of 1.577 Å, so that the ethylene double bond is changed to single bond. In the same way the Cβ–Cγ distance stretches to a value of 1.576 Å indicating the formation of new C–C bond.

The hydrogen insertion product (**2d**) showed the formation of the Zr–H bond (1.820 Å) and the rupture of the Zr–C3 bond (2.779 Å). Also observed is the rupture of the hydrogen molecule (H1–H2 distance 3.410 Å), so that the hydrogen insertion reaction results in a termination chain process forming saturated polymer chains.

After the ethylene insertion into Cp_2ZrH^+, the formed product (**3d**) presents a strong β-agostic interaction (Zr–Hβ distance 2.207 Å and ZrCαCβ angle 86.3°). The formation of a Zr–C bond was also observed. This product could insert successive ethylene monomers yielding a polymer chain.

3.2. Energies

The energy profiles for both ethylene and hydrogen insertions in $Cp_2ZrCH_3^+$ are shown in Figs. 1 and 2, respectively, while the energy profile for ethylene insertion into Cp_2ZrH^+ is shown in Fig. 3. All energies are relative to reactants.

In Fig. 1 the energy profile for the ethylene insertion into the metal–alkyl bond of reactant (**1a**) is displayed. As can

Table 4
Thermodynamic data for all reaction steps (the labels are shown in Figs. 1–3). All energies are in kcal/mol, except entropy in cal/mol K. All calculations have been performed to $T = 290.15$ K and $P = 1$ atm (except $\Delta E_{elect} T = 0$ K). The imaginary frequencies of the transition states have been neglected. The energy increments have been calculated according to $A \rightarrow B$ $\Delta E = E_B - E_A$

Steps	ΔE_{elec} [a]	ΔE_{tot} [b]	ΔH_{total} [c]	ΔG_{total} [d]	ΔS_{total} [e]	Imaginary frequencies (cm^{-1})
1a+ethylene → **1b**	−18.27	−15.90	−16.49	−5.41	−37.20	–
1b → **1c**	+7.48	+7.48	+7.48	+10.55	−10.30	−298.7
1c → **1d**	−7.14	−5.59	−5.59	−3.09	−8.40	–
2a + hydrogen → **2b**	−6.76	−4.68	−5.25	+1.52	−23.70	–
2b → **2c**	+4.58	+4.43	+4.43	+6.70	−7.59	−848.3
2c → **2d**	−15.03	−12.28	−12.28	−11.99	−0.96	–
3a → **3d**	−37.88	−33.82	−34.42	−22.85	−38.99	–

[a] Electronic energy.
[b] Electronic energy plus zero point energy energy and thermal corrections.
[c] $\Delta H_{total} = \Delta E_{total} + RT$.
[d] $\Delta G_{total} = \Delta H_{total} - T\Delta S_{total}$.
[e] Entropy increment.

be seen, the interaction binding energy of the ethylene to Cp_2ZrCH_3 (**1a**) is an exothermic reaction (−18.27 kcal/mol). The energy barrier for ethylene insertion into Zr–Cα bond is 7.48 kcal/mol. This value is comparable with other theoretical values [7,13] and in agreement with the estimated experimental propagation barriers for ethylene polymerization with metallocene catalysts (5–8 kcal/mol) [45–47]. The global reaction energy from reactants (**1a**) to products (**1d**) is very exothermic (−25.41 kcal/mol). The relatively small energy barrier along with large exothermicity explain the experimental fact that metallocenes are very active catalysts.

In Fig. 2 the energy profile of the insertion reaction of hydrogen into the metal–alkyl bond of reactant (**1a**) is shown. The interaction binding energy of the hydrogen molecule to reactant $Cp_2ZrCH_3^+$ (**1a**) is exothermic with 6.76 kcal/mol. Comparing the interaction binding energies for ethylene and hydrogen to reactant $Cp_2ZrCH_3^+$ (**1a**) it might be observed that the hydrogen π-complex (**2b**) is less stable than the ethylene π-complex (**1b**) by 11.51 kcal/mol.

The energy barrier found for the hydrogen insertion into $Cp_2ZrCH_3^+$ (**1a**) is 4.58 kcal/mol, approximately 3 kcal/mol lower than the barrier for the ethylene insertion. These results indicate that the hydrogen insertion into Zr–C bond is more favored than the ethylene insertion, which are in agreement with the experiment findings published, showing that the rate constants for the hydrogen insertion is higher than the corresponding ethylene insertion [48]. In addition, this observation is in agreement with the experimental results obtained by Blom and Dahl [24] for ethylene polymerization in the presence of hydrogen. They observed that the hydrogen disappeared at the beginning of the polymerization reaction showing a higher reactivity of hydrogen to the $Cp_2ZrCl_2/MAO/SiO_2$ catalysts, explaining the experimental observation of the decrease of molecular weight of polymers in presence of hydrogen [14–27].

The global exothermicity of the hydrogen insertion is 21.79 kcal/mol while the global exothermicity of the ethylene insertion was 25.41 kcal/mol, therefore the product (**1d**) is expected to be the most likely thermodynamic product. On the other hand, the energy barrier for the hydrogen insertion is lower than the ethylene insertion (4.58 vs 7.48 kcal/mol) suggesting that the structure (**2d**) is the most probable kinetic product.

The energy profile for the ethylene insertion into the hydride complex formed by hydrogenolysis (Cp_2ZrH^+, **3a**) is shown in Fig. 3. This reaction was studied in order to see whether the reinitiation of a new polymer chain after the hydrogenolysis reaction is possible. Along the reaction coordinate, no stationary points were found. This insertion reaction takes place without energy barrier from reactants (**3a**) to products (**3d**) and exhibits a large exothermicity (37.88 kcal/mol). Similar results have been reported for the acetylene insertion into the Cl_2ZrH^+ species [29] and ethylene insertion into H_2TiH^+ [28]. All these findings suggest that the ethylene insertion into the hydride complex is an easy process and therefore the initiation of the new polymer chain is possible after the hydrogenolysis has taken place.

From the experimental point of view, it still remains unclear whether the presence of hydrogen affects the catalytic activity or not [24,25]. Based on our calculations, it seems to be that the presence of hydrogen could not be responsible for an eventual decrease of the polymerization rate.

3.3. Thermodynamic calculations

Thermodynamic data calculated at room temperature are collected in Table 4. All energies were obtained following the standard statistical thermodynamic procedures implemented in GAUSSIAN98 [30]. Details of the calculation are given in Section 2. This calculation corresponds to the thermodynamic equilibrium.

The activation energy found for the hydrogen insertion

into $Cp_2ZrCH_3^+$ (**1a**) is smaller than that corresponding to the ethylene insertion (4.58 vs 7.48 kcal/mol), as discussed in Section 3.2. Taking into account only this factor, the hydrogen insertion should be more probable than the ethylene and therefore the ethylene polymerization could not take place in the presence of hydrogen which is opposite to the experimental findings [24–27]. Let us analyze this discrepancy. The binding complex should be stabilized prior to the insertion process into the Zr–C bond. The formation of this complex is much more favorable in the case of ethylene insertion than the hydrogen insertion (see Figs. 1 and 2). Therefore, by assuming that the number of molecules of ethylene and hydrogen are the same, the population in the π-ethylene complex should be higher than in the dihydrogen complex. By using Boltzmann statistics the population ratio between ethylene π-complex (**1b**) and dihydrogen complex (**2b**) can be calculated using the following equation:

$$\frac{n_{1b}}{n_{2b}} = \frac{\exp(-\Delta G_{1a+\text{Ethylene}\rightarrow 1b}/RT)}{\exp(-\Delta G_{1a+\text{Hydrogen}\rightarrow 2b}/RT)}$$

where n_{1b} and n_{2b} are the populations in the ethylene and hydrogen complexes, respectively. The population ratio is 1.2×10^5. Furthermore, taking into account this population ratio and the free energy barriers ($\Delta G^{\#}$) in kcal/mol it is possible to calculate the probability ratio of ethylene to hydrogen insertion, according to the following equation:

$$\frac{P_{C_2H_4}}{P_{H_2}} = \frac{1.20 \times 10^5 \exp(-\Delta G^{\#}_{1b\rightarrow 1c}/RT)}{\exp(-\Delta G^{\#}_{2b\rightarrow 2c}/RT)}$$

A probability of 180 ethylene per hydrogen insertions (chain termination reaction) was found, which correspond to oligomers with molecular weights of about 5000 g/mol. As the hydrogen is consumed, it is expected that the molecular weight of the chains increase. Molecular weights of 20 500 and 50 000 g/mol were calculated when 75 and 90% of hydrogen have been consumed, respectively. Therefore, on the one hand a broadening of the molecular weight distribution in the presence of hydrogen is expected from these theoretical results, which is in agreement with the experimental data published by Bloom et al. [24]. On the other hand these authors found that low molecular weight oligomers are produced at the beginning of the reaction and also that at the end of the polymerization, polyethylene with higher molecular weights of about 40 000 g/mol ($\overline{M_w}$) is obtained. Therefore, all the theoretical results are in reasonable agreement with the experimental observations.

4. Conclusions

From the above-presented results, we can conclude the following points:

1. The hydrogenolysis process is an effective chain-termination mechanism in the polymerization catalyzed by metallocene complexes. The insertion of a hydrogen molecule into the metal–alkyl bond shows a small energy barrier (4.5 kcal/mol) which is even lower than that corresponding to the ethylene insertion (7.5 kcal/mol). These data support the experimental findings of the early hydrogen consumption during the hydrogenolysis batch process [24]. Although the energy barrier for the ethylene insertion is higher than that corresponding to the hydrogen insertion, the polymerization reaction is still possible due to the fact that ethylene forms a reactant complex (**1b**) much more stable than the corresponding dihydrogen complex (**2b**). Therefore, the population in **1b** is higher that **2b**, thus increasing the probability of ethylene (180 insertions) per hydrogen insertion.
2. The thermodynamic analysis gives a reasonable account of the oligomeric species experimentally found at the beginning of the ethylene polymerization in the presence of hydrogen when the process is performed in batch mode [24]. The thermodynamic calculations reported oligomeric molecular weights of about 5000 g/mol. The thermodynamic calculations suggest that the molecular weight gradually increases with the hydrogen consumption (20 500 g/mol for 75% of the consumed hydrogen, and 50 000 g/mol for the 90% of the consumed hydrogen). This result is in agreement with the experimental fact that polymer molecular weight gradually increases until there is no hydrogen left [24].
3. The formation of chains with lower molecular weights is observed when the ethylene polymerization is performed in the presence of hydrogen during the first steps with respect to the polymerization reaction in the absence of hydrogen. It is evident that when no hydrogen remains in the reactor the formed polymer will have the same molecular weight as if no hydrogen were present at all. Therefore, a broadening of molecular weight distribution is expected from both experimental [24–27] and theoretical results.
4. The energetic data obtained in the present work are indicative that the presence of molecular hydrogen does not slow down the polymerization reaction catalyzed by zirconocene at least from the viewpoint of the hydrogen molecule insertion and reactivation of the hydride catalyst. The initiation of a new polymer chain from the organometallic hydride formed after hydrogenolysis is a spontaneous process as deduced from the absence of any energy barrier during the insertion of ethylene.

Acknowledgements

Thanks are due to the CAM (Grant I + D058/94) for the support of this investigation. One of us (J.R.) wishes to thank CICYT for the tenure of a fellowship. The authors also acknowledge Repsol S.A. for the permission to publish these data.

References

[1] Jolly CA, Marynick DS. J Am Chem Soc 1989;111:7968.
[2] Weiss H, Ehrig M, Ahlrichs R. J Am Chem Soc 1994;116:4919.
[3] Meier RJ, Van Doremaele GHJ, Iarlori S, Buda F. J Am Chem Soc 1994;116:7274.
[4] Margl P, Lohrentz JCW, Ziegler T, Blöchl PE. J Am Chem Soc 1996;118:4434.
[5] Lohrentz JCW, Woo TK, Ziegler T. J Am Chem Soc 1995;117:12 793.
[6] Lohrentz JCW, Woo TK, Fan L, Ziegler T. J Organomet Chem 1995;497:91.
[7] Yoshida T, Koga N, Morokuma K. Organometallics 1995;14:746.
[8] Woo TK, Fan L, Ziegler T. Organometallics 1994;13:2252.
[9] Kawamura-Kuribayashi H, Koga N, Morokuma K. J Am Chem Soc 1992;114:8687.
[10] Cruz VL, Muñoz-Escalona A, Martinez-Salazar J. J Polym Sci A: Polym Chem 1998;36:1157.
[11] Cruz VL, Muñoz-Escalona A, Martinez-Salazar J. Polymer 1996;37:1663.
[12] Woo TK, Margl PM, Lohrenz JCW, Blöchl PE, Ziegler T. J Am Chem Soc 1996;118:13 021.
[13] Muñoz-Escalona A, Ramos J, Cruz VL, Martinez-Salazar J. J Polym Sci Part A: Polym Chem 2000; in press.
[14] Guastalla G, Giannini U. Makromol Chem, Rapid Commun 1983;4:519.
[15] Chadwick JC, Van Kessel GMM, Sudmeijer O. Macromol Chem Phys 1995;196:1431.
[16] Bukatok GD, Goncharov VS, Zakharov VA. Macromol Chem Phys 1995;196:1751.
[17] Chanwick JC, Morini G, Albizzati E, Balbontin G, Mingozzi I, Cristofori A, Sudmeijer O, Van Kessel GMM. Macromol Chem Phys 1996;197:2501.
[18] Soares JBP, Hamielec AE. Polymer 1996;37:4599 and references therein.
[19] Kojoh S, Kioka M, Kashiwa N, Itoh M, Mizuno A. Polymer 1995;36:5015.
[20] Mori H, Tashino K, Terano M. Macromol Chem Phys 1995;196:651.
[21] Carvill A, Tritto I, Locatelli P, Sachhi MC. Macromolecules 1997;30:7056.
[22] Jüngling S, Mülhaupt R, Stehling U, Brintzinger H, Fischer D, Langauser F. J Polym Sci Part A: Polym Chem 1995;33:1305.
[23] Tsutsui T, Kashiwa N, Mizuno A. Makromol Chem, Rapid Commun 1990;11:565.
[24] Blom R, Dahl IM. Macromol Chem Phys 1999;200:442.
[25] Kaminsky W, Lüker H. Makromol Chem, Rapid Commun 1984;5:225.
[26] Chien JCW, Wang B. J Polym Sci Part A: Polym Chem 1990;28:15.
[27] D'Agnillo L, Soares JBP, Penlidis A. Macromol Chem Phys 1998;199:955.
[28] Zakharov II, Zakharov VA, Zhidomirov GM. Kinet Catal 1994;35:64.
[29] Hyla-Kryspin I, Niu S, Gleiter R. Organometallics 1995;14:964.
[30] Frisch MJ, Trucks GW, Schlegel HB, Scuseria GE, Robb MA, Cheeseman JR, Zakrzewski VG, Montgomery JA, Stratmann RE, Burant JC, Dapprich S, Millan JM, Daniels AD, Kudin KN, Strain MC, Farkas O, Tomasi J, Barone V, Cossi M, Cammi R, Mennucci B, Pomelli C, Adamo C, Clifford S, Petersson GA, Ayala PY, Cui Q, Morokuma K, Malick DK, Rabuk AD, Raghavachari K, Foresman JB, Ciolowski J, Ortiz JV, Stefanov BB, Liu G, Liashenko A, Piskorz P, Komaromi I, Gomperts R, Martin RL, Fox DJ, Keith TA, Al-Laham MA, Peng CY, Nanayakkara A, Gonzalez C, Challacombe M, Gill PMW, Johnson BG, Chen W, Wong MW, Andres JL, Head-Gordon M, Reploge ES, Pople JA. GAUSSIAN98 (Revision A.1), Gaussian Inc., Pittsburgh, PA, 1998.
[31] Becke AD. J Chem Phys 1993;98:5648.
[32] Froese RDJ, Musaev DG, Matsubara T, Morokuma K. J Am Chem Soc 1997;119:7190.
[33] Vosko H, Wilk L, Nusair M. Can J Phys 1980;58:1200.
[34] Lee, Yang W, Parr RG. Phys Rev B 1988;37:785.
[35] Slater JC. Quantum theory of molecular and solids. Vol. 4: the self-consistent field for molecular and solids. New York: McGraw-Hill, 1974.
[36] Becke AD. Phys Rev A 1988;38:3098.
[37] Hay PJ, Wadt WR. J Chem Phys 1985;82:270.
[38] Wadt WR, Hay PJ. J Chem Phys 1985;82:284.
[39] Hay PJ, Wadt WR. J Chem Phys 1985;82:299.
[40] Peng C, Schlegel HB. Isr J Chem 1993;33:449.
[41] Spartan version 5.1.1 Wavefunction, Inc. 18401 Von Karman Avenue, Suite 370. Irvine, CA 92612, USA.
[42] Yang X, Stern CL, Marks TJ. J Am Chem Soc 1991;113:3623.
[43] Arlman EJ, Cossee P. J Catal 1964;3:99.
[44] Brookhart M, Green MLH. J Organomet Chem 1983;250:395.
[45] Natta G, Zambelli A, Pasquon I, Giongo GM. Chim Ind 1996;48:1298.
[46] Chien JCW, Razavi A. J Polym Sci Part A: Polym Chem 1988;26:2369.
[47] Chien JCW, Sugimoto RJ. J Polym Sci Part A: Polym Chem 1991;29:459.
[48] Alameddin NG, Ryan MF, Eyler JR, Siedle AR, Richardson DE. Organometallics 1995;14:5005.